Hindawi Publishing Corporation
International Journal of Photoenergy
Volume 2013, Article ID 435017, 7 pages
http://dx.doi.org/10.1155/2013/435017

Research Article

Degradation of Pesticide Chlorothalonil by Visible Light-Responsive Photocatalyst Ferrioxalate and H_2O_2 under Solar Irradiation

Malay Chaudhuri, Hafizi Zuhali, and Augustine Chioma Affam

Department of Civil Engineering, Universiti Teknologi PETRONAS, Bandar Seri Iskandar, 31750 Tronoh, Perak, Malaysia

Correspondence should be addressed to Malay Chaudhuri; malaychaudhuri@yahoo.com

Received 18 January 2013; Revised 17 April 2013; Accepted 18 April 2013

Academic Editor: Leonardo Palmisano

Ferrioxalate is a visible light-responsive photocatalyst. The solar ferrioxalate/H_2O_2 process has high degradation efficiency because ferrioxalate is able to absorb light strongly at longer wavelength and generates hydroxyl radical with high quantum yield. Degradation of pesticide chlorothalonil in aqueous solution by ferrioxalate/H_2O_2 under solar irradiation was examined. The optimum operating conditions for treatment of a 300 mg/L chlorothalonil aqueous solution were obtained by using the central composite design of the response surface methodology. Under the optimum operating conditions (H_2O_2/COD molar ratio 2.75, H_2O_2/Fe^{3+} molar ratio 75, $H_2O_2/C_2H_2O_4$ molar ratio 37.5, reaction time 90 min, and pH 3), COD, NH_3-N, and TOC removal of 75.71, 47.11, and 54.33%, respectively, was achieved and the biodegradability (BOD_5/COD ratio) improved from zero to 0.42. Model prediction and actual removal were in close agreement (<4% error). The solar ferrioxalate/H_2O_2 process is effective in pretreatment of the chlorothalonil aqueous solution for biological treatment.

1. Introduction

Chlorothalonil is a broad-spectrum of organochlorine pesticide (fungicide) used to prevent foliar diseases in vegetable and ornamental crops in agricultural fields [1] and belongs to class IV of the World Health Organization classification of pesticides [2]. It is classified as a probable carcinogen, and the 4-hydroxy chlorothalonil transformation product is more soluble, more stable, and, for some species, more toxic than its parent compound [3]. Chlorothalonil has the potential to contaminate water bodies adjacent to its point of use by spray drift, runoff, or sediment transport. Chlorothalonil has been detected in surface water [4, 5], inland waterways [6], natural water [7], rainfall [8], and air samples [9] generally adjacent to agricultural areas where it was applied. Chlorothalonil is sufficiently persistent to undergo long-range atmospheric transport on a regional scale [10] and can also exhibit chemical stability and resistance to biodegradation [11–13]. Reports have indicated that a minimum of 50 μg/L concentration of pesticide is toxic to guppy fish [14].

Advanced oxidation processes (AOPs) constitute a promising technology for the treatment of water and wastewater containing recalcitrant organic compounds with high toxicity and low biodegradability [15]. Oxidation technologies have shown that a partial oxidation of toxic water may increase its biodegradability [16, 17]. Oxidation with Fenton's reagent is based on hydroxyl radical ($OH^\bullet$) produced by catalytic decomposition of hydrogen peroxide (H_2O_2) in reaction with ferrous ion (Fe^{2+}) [18]. In the photo-Fenton process, the rate of $OH^\bullet$ radical formation is increased by photoreactions of H_2O_2 and/or Fe^{3+} that produce $OH^\bullet$ radical directly or regenerate Fe^{2+} [19], thus increase the efficiency of the process. Ferrioxalate is a visible light-responsive photocatalyst. The solar ferrioxalate/H_2O_2 process has high degradation efficiency because ferrioxalate is able to absorb light strongly at longer wavelength and generates $OH^\bullet$ radical with high quantum yield [20]. The quantum yield of Fe^{2+} regeneration greatly increases when Fe^{2+} complexes with a carboxylic anion, such as oxalate [21]. The ferrioxalate complex, $Fe^{III}(C_2O_4)_3^{3-}$,

is highly photosensitive, and reduction of Fe^{3+} to Fe^{2+}, through a photo-induced ligand to metal charge transfer, can occur over the ultraviolet and into the visible (out to $\lambda \sim 550$ nm):

$$Fe^{III}(C_2O_4)_3^{3-} + h\nu \longrightarrow Fe^{2+} + 2C_2O_4^{2-} + C_2O_4^{\bullet -} \quad (1)$$

$$C_2O_4^{\bullet -} \longrightarrow CO_2^{\bullet -} + CO_2 \quad (2)$$

$$CO_2^{\bullet -} + Fe^{III}(C_2O_4)_3^{3-} \longrightarrow Fe^{2+} + CO_2 + 3C_2O_4^{2-} \quad (3)$$

The reactions can be collapsed into one reaction, since the short lifetime of the oxyl radical, $C_2O_4^{\bullet -}$, should preclude it from participation in other reactions, and its decarboxylation product, $CO_2^{\bullet -}$, is not involved in any other significant reactions:

$$Fe^{III}(C_2O_4)_3^{3-} + h\nu \longrightarrow Fe^{2+} + CO_2 + 2.5C_2O_4^{2-} \quad (4)$$

There are no other significant photochemical reactions (e.g., H_2O_2 photolysis) because the molar extinction coefficients of the reactants are such that ferrioxalate is the predominant absorber. The Fe^{2+} produced then generates $OH^{\bullet}$ radical via the Fenton reaction:

$$Fe^2 + H_2O_2 + 3C_2O_4^{2-} \longrightarrow Fe^{III}(C_2O_4)_3^{3-} + OH^- + OH^{\bullet} \quad (5)$$

In the presence of a sufficient excess of oxalate, Fe^{3+} will coordinate with either two or three oxalate ligands. As with the photo-Fenton reaction, iron cycles between oxidation states and the production of hydroxyl radical is limited only by the availability of light, H_2O_2, and oxalate, the latter two of which are depleted during the reaction. UV-vis/ferrioxalate/H_2O_2 treatment of aniline wastewater [22], dyehouse waste [23], reactive dyes [24], orange II [25], and phenolic pollutants [26] have been reported. There is no report on degradation of pesticide chlorothalonil by solar ferrioxalate/H_2O_2 process.

The present study examined degradation of pesticide chlorothalonil in aqueous solution by solar ferrioxalate/H_2O_2 process in terms of chemical oxygen demand (COD), ammonia nitrogen (NH_3-N) and total organic carbon (TOC) removal, and biodegradability (BOD_5/COD ratio) improvement. The treatment was optimized by using the central composite design (CCD) of the response surface methodology (RSM).

2. Materials and Methods

2.1. Chemicals and Pesticide. Hydrogen peroxide (30%, w/w), oxalic acid ($C_2H_2O_4 \cdot 2H_2O$), and ferric sulfate ($Fe_2(SO_4)_3$) were purchased from R&M Marketing, Essex, UK. The pesticide chlorothalonil used to prepare aqueous solution was obtained from a commercial source and was used as received. Figure 1 shows the chemical structure of chlorothalonil.

2.2. Analytical Methods. Chemical oxygen demand (COD) was determined according to Method 5220D (closed reflux, colorimetric method) of the Standard Methods [27], where the sample contained hydrogen peroxide (H_2O_2), to reduce interference in COD determination, pH was increased to above 10 so as to decompose hydrogen peroxide to oxygen and water [28, 29]. TOC analyzer (Model 1010, O & I Analytical) was used for determining total organic carbon (TOC). The pH was measured by a pH meter (HACH sension 4) and a pH electrode (HACH platinum series pH electrode model 51910, HACH Company, USA). Biodegradability was measured by 5-day biochemical oxygen demand (BOD_5) test according to Method 5210B (seeding procedure) of the Standard Methods [27]. The treated pesticide aqueous solution was adjusted to pH 7 before the BOD_5 test. Ammonia nitrogen (NH_3-N) was measured by the Nessler method [30]. DO was measured using YSI 5000 dissolved oxygen meter. The seed for the BOD_5 test was obtained from a municipal wastewater treatment plant.

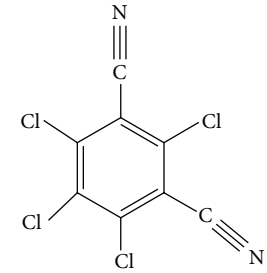

Figure 1: Chemical structure of chlorothalonil.

2.3. Chlorothalonil Aqueous Solution. Chlorothalonil aqueous solution was 300 mg/L of chlorothalonil in distilled water. It was prepared weekly and stored at 4°C. The characteristics of the aqueous solution were COD 350 mg/L, NH_3-N 1.58 mg/L, and TOC 94.49 mg/L. The high chlorothalonil concentration was chosen to reflect the concentration in pesticide-manufacturing wastewater and to explore the oxidation potential of the ferrioxalate/H_2O_2 process.

2.4. Experimental Procedure. Batch experiments were conducted with 200 mL of chlorothalonil aqueous solution in a 250 Pyrex beaker, placed in a SolSim solar simulator photoreactor (Luzchem Research Inc., Gloucester, ON, Canada), with solar intensity 0.85 kW/m^2. The required amount of $C_2H_2O_4$ and Fe^{3+} was added to the aqueous solution and mixed by a magnetic stirrer to ensure complete homogeneity during reaction. Thereafter, necessary amount of H_2O_2 was added to the mixture with simultaneous adjustment to pH 3 by using H_2SO_4. The time at which H_2O_2 was added to the mixture was considered as the beginning of the experiment. Samples were taken at preselected time intervals and filtered through 0.45 μm membrane filter for determination of COD, NH_3-N, and TOC, and when required BOD_5.

2.5. Optimization and Response Surface Modeling . Design expert software Version 6.0.7 [31] was used for statistical design of experiment and data analysis. Central composite

Table 1: Experimental design and predicted and actual removal.

Experimental design				Removal (%)					
				COD		NH_3-N		TOC	
A: H_2O_2/COD (molar ratio)	B: H_2O_2/Fe^{3+} (molar ratio)	C: $H_2O_2/C_2H_2O_4$ (molar ratio)	D: Time (min)	Predict	Actual	Predict	Actual	Predict	Actual
4.00	100.00	25.00	120.00	67.89	71.14	46.11	52.11	46.10	50.00
2.75	25.00	37.50	90.00	69.45	67.14	49.00	43.23	35.16	28.00
1.50	50.00	25.00	120.00	70.85	68.57	46.26	44.00	40.54	41.16
2.75	75.00	37.50	150.00	73.14	73.54	41.17	40.47	63.49	60.11
4.00	100.00	50.00	60.00	67.18	69.15	40.60	41.81	44.25	45.08
4.00	100.00	50.00	120.00	67.04	60.00	48.29	49.11	42.79	44.44
2.75	75.00	37.50	90.00	72.71	75.14	44.81	43.29	52.20	49.11
1.50	100.00	25.00	60.00	61.42	66.93	58.30	62.00	34.23	40.44
1.50	100.00	25.00	120.00	69.36	67.42	47.57	43.00	61.57	57.31
2.75	75.00	37.50	90.00	72.71	72.00	44.81	49.60	52.20	53.44
2.75	75.00	62.50	90.00	71.69	70.85	45.93	44.44	52.33	51.16
4.00	50.00	50.00	60.00	64.08	65.71	35.33	35.00	61.77	70.11
2.75	75.00	37.50	90.00	72.71	69.71	44.81	40.00	52.20	55.50
1.50	100.00	50.00	60.00	61.37	61.14	51.39	52.40	34.23	30.11
4.00	50.00	25.00	60.00	64.93	61.42	38.82	34.50	56.82	57.11
2.75	125.00	37.50	90.00	71.07	74.00	54.81	50.00	38.67	40.30
4.00	50.00	25.00	120.00	63.22	63.14	40.91	40.00	46.81	55.00
1.50	50.00	50.00	60.00	64.41	60.85	45.00	37.95	30.73	29.00
1.50	50.00	50.00	120.00	78.18	78.00	46.25	49.11	47.53	54.00
2.75	75.00	37.50	90.00	72.71	75.14	44.81	43.11	52.20	50.00
4.00	50.00	50.00	120.00	68.80	74.00	41.20	36.44	50.76	46.00
5.25	75.00	37.50	90.00	57.78	56.85	35.45	35.00	47.91	43.00
4.00	100.00	25.00	60.00	74.46	74.28	47.21	44.44	47.28	44.88
1.50	100.00	50.00	120.00	70.22	73.42	49.44	52.70	60.58	61.75
0.25	75.00	37.50	90.00	59.59	61.14	53.00	51.39	31.63	31.00
2.75	75.00	12.50	90.00	71.68	73.14	52.55	55.00	48.37	44.00
2.75	75.00	37.50	30.00	66.40	67.42	41.02	42.67	47.16	45.00
2.75	75.00	37.50	90.00	72.71	70.00	44.81	44.11	52.20	56.12
1.50	50.00	25.00	60.00	63.55	70.28	53.80	53.07	22.75	25.17
2.75	75.00	37.50	90.00	72.71	74.28	44.81	48.77	49.00	52.20

design (CCD) of the response surface methodology (RSM) was used to optimize the operating conditions (variables) of the treatment because it is well suited for fitting a quadratic surface, which usually works well for process optimization, and it is the experimental design mostly utilized for the development of analytical procedure as against three-level factorial design which is not frequently used and has been limited to the optimization of two variables [32]. The variables were simultaneously changed in a central composite circumscribed design. The values of the variables H_2O_2/COD molar ratio, H_2O_2/Fe^{3+} molar ratio, $H_2O_2/C_2H_2O_4$ molar ratio, and reaction time were set at three levels: −1 (low), 0 (central) and +1 (high), and the total number of experiments with three factors was obtained as 30 ($2^k + 2k + 6$), where k is the number of factors (which equals 4 in this case). Twenty four experiments were augmented with six replications at the design center to evaluate the pure error and carried in randomized order as required in the circumscribed composite design. The variables H_2O_2/COD molar ratio, H_2O_2/Fe^{2+} molar ratio, $H_2O_2/C_2H_2O_4$ molar ratio, and reaction time were studied in the range 1.5–4.0, 25–50, 50–100, and 60–120 min, respectively. Chosen response parameters for the process were removal of COD, NH_3-N, and TOC. Table 1 shows the experimental design and the predicted response (removal). Regression models and statistical analysis, contour plots normal probability and plots were made. Model terms were evaluated by the P value (probability) with 95% confidence level. The quality of fit of the polynomial model was expressed by the coefficient of determination R^2. The optimum operating conditions (variables) were identified from the contour plots and response equation simultaneously. The following response equation

Table 2: ANOVA of the response parameters.

Parameter	F-test	P value	R^2	Adequate precision (A.P)
COD	2.63	0.0001	0.8031	11.992
NH_3-N	2.88	0.0001	0.7579	11.320
TOC	6.54	0.0001	0.8196	15.546

describing an empirical second-order polynomial model was used to assess the predicted results:

$$Y = \beta_o + \sum_{i=1}^{k}\beta_i x_i + \sum_{i=1}^{k}\beta_{ii}x_1^2 + \sum_{i=1}^{k}\sum_{j=1}^{k}\beta_{ij}x_i x_j + \varepsilon, \quad (6)$$

where Y is the dependent response; β_o is the constant coefficient; i, ii, and ij are the coefficients for the linear, quadratic, and interaction effect; x_i and x_j are the factors (i.e., H_2O_2/COD, H_2O_2/Fe^{3+}, and $H_2O_2/C_2H_2O_4$ molar ratio and reaction time); k signifies the number of independent variables, and ε is the random error [32]. The result (Y) was calculated as the sum of a constant (β_o), four first-order effects (A, B, C, and D), four second-order effects (A^2, B^2, C^2, and D^2) and four interaction effects (AB, AC, BD, and CD).

3. Results and Discussion

Based on the experimental design, predicted and actual removal (average of triplicate experimental results) are shown in Table 1.

3.1. Regression Models and Statistical Analysis. To ascertain the suitability of the regression model, assess the interaction between the independent variables (operating conditions) and the dependent variables (responses), and subsequently obtain the "goodness of fit", analysis of variance (ANOVA) was performed. Fisher F-test value, P-value, coefficient of determination R^2, and adequate precision (A.P) are shown in Table 2. F-test value is a measure of variation of the data about the mean [26]. A P-value less than 0.05 indicates the suitability of the proposed models for treatment as there is no lack-of-fit. The models for COD, NH_3-N, and TOC removal (Y_1, Y_2, and Y_3) were significant by the F-test at 95% confidence level employed as all responses had a P-value < 0.05, and therefore the removal fits the data well. The coefficient of determination (R^2) is the proportion of variability in a data set which indicates whether the empirical model is good enough for the quadratic fit to navigate the design space defined by the CCD [27]. The R^2 value gives the proportion of the total variation in the response predicted by the model to the actual data. The R^2 values were 0.8031 (COD), 0.7579 (NH_3-N), and 0.8196 (TOC). Adequate precision (A.P.) ratio compares the range of the predicted value at the design points to the average prediction error. Ratios greater than 4 indicate adequate model discrimination and can be used to navigate the design space defined by the CCD [27]. The A.P. for all the responses was greater than 4. The ANOVA results indicate adequate agreement between the model prediction and actual removal. The following fitted regression models were obtained to quantitatively investigate the effects of A: H_2O_2/COD molar ratio, B: H_2O_2/Fe^{3+} molar ratio, C: $H_2O_2/C_2H_2O_4$ molar ratio, and D: reaction time on COD, NH_3-N, and TOC removal, respectively.

COD removal,

$$\begin{aligned} Y_1 = {} & 74.68 - 1.03A + 0.34B - 0.19C + 3.17D \\ & - 4.16A^2 - 1.22B^2 - 0.79C^2 \pm 0.43D^2 + 2.36AB \\ & + 0.68\,AC - 0.11BD + 3.35CD. \end{aligned} \quad (7)$$

NH_3-N removal,

$$\begin{aligned} Y_2 = {} & 43.88 - 3.73A + 3.52B - 2.12C - 0.75D \\ & - 0.43A^2 + 0.96B^2 + 2.12C^2 - 8.437E - 003D^2 \\ & + 1.40AB + 0.40\,AC + 1.98AD + 0.18BC \\ & - 1.01BD + 3.49CD. \end{aligned} \quad (8)$$

TOC removal,

$$\begin{aligned} Y_3 = {} & 51.19 + 4.81A - 1.76B + 1.08C + 3.84D \\ & - 3.59A^2 - 1.52B^2 - 0.98C^2 + 0.35D^2 - 6.35AB \\ & - 0.73\,AC - 6.85AD - 2.76BC + 2.65BD + 0.51CD. \end{aligned} \quad (9)$$

In (7), (8), and (9), the values of the sum of a constant (β_o), (74.68, 43.88, and 51.19) represent the percentage removal of COD, NH_3-N, and TOC, respectively. The positive sign indicates that the variable is directly proportional to the response (COD, NH_3-N, and TOC removal), and the negative sign indicates that the variable is inversely proportional to the response.

3.2. Process Analysis. Visualization of the predicted model equation can be obtained from the contour plot [25]. A contour plot is a two-dimensional display of the surface plot, and, in the contour plot, lines of constant response are drawn in the plane of the variables. The contour plot helps to visualize the shape of a response surface. When the contour plot displays ellipses or circles, the center of the system refers to a point of maximum or minimum response. Sometimes, contour plot may display hyperbolic or parabolic system of the contours [28]. Figures 2, 3, and 4 show the contour plots for COD, NH_3-N, and TOC removal. Decreasing oxalate (increasing $H_2O_2/C_2H_2O_4$ molar ratio) and increasing H_2O_2 (increasing H_2O_2/COD molar ratio) will reduce COD removal, increasing oxalate (decreasing $H_2O_2/C_2H_2O_4$ molar ratio) and increasing H_2O_2 (increasing H_2O_2/COD molar ratio) will reduce NH_3-N removal, and increasing oxalate (decreasing $H_2O_2/C_2H_2O_4$ molar ratio) and decreasing H_2O_2 (decreasing H_2O_2/COD molar ratio)

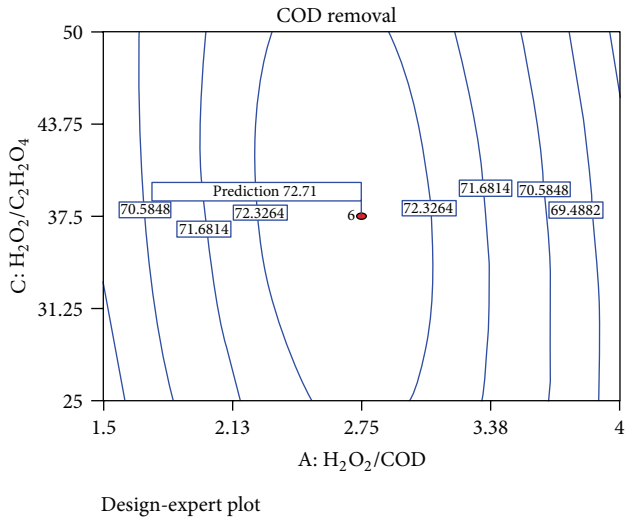

FIGURE 2: Contour plot for COD removal.

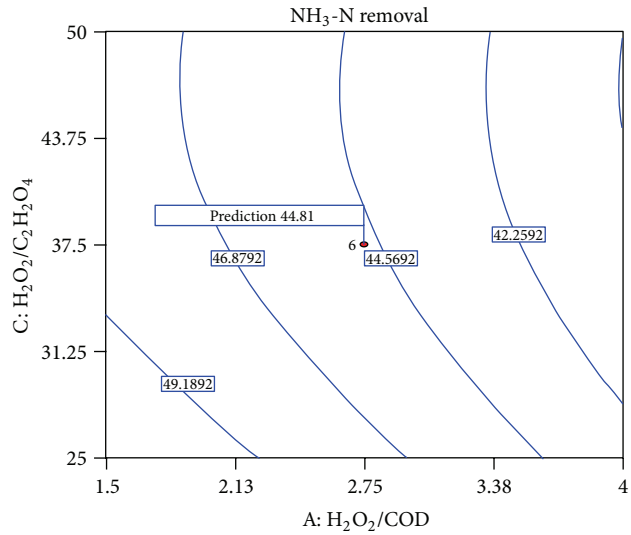

FIGURE 3: Contour plot for NH_3-N removal.

simultaneously or one at a time will reduce TOC removal at H_2O_2/Fe^{3+} molar ratio 75.0 and reaction time 90 min in all three cases. The adequacy of the models was also evaluated by the residuals that is, difference between the predicted and the actual response value. Plot of predicted versus actual removal (Figures 5, 6, and 7) indicates that there is no abnormalities in the model as all data were found around the line of "best fit".

3.3. Optimization and Model Verification. Numerical optimization was used to determine the optimum operating conditions for COD, NH_3-N, and TOC removal. Based on the response surface and desirability functions (figure not shown), the optimum operating conditions were obtained. In this case, all responses were targeted to be in range and were goaled to be maximized. The optimum conditions were obtained for highest desirability at H_2O_2/COD molar ratio 2.75, H_2O_2/Fe^{3+} molar ratio 75, $H_2O_2/C_2H_2O_4$ molar ratio 37.5, and reaction time 90 min at pH 3. Under the operating conditions, 72.71, 45.47, and 52.20% removal of COD, NH_3-N, and TOC, respectively, was predicted based on desirability function of 1.00 (Table 3). Actual removal under the optimum operating conditions is shown in Table 3. The model prediction and actual removal were in close agreement (<4% error).

3.4. Biodegradability. Under the optimum operating conditions (H_2O_2/COD molar ratio 2.75, H_2O_2/Fe^{3+} molar ratio 75, $H_2O_2/C_2H_2O_4$ molar ratio 37.5, reaction time 90 min, and pH 3), solar ferrioxalate/H_2O_2 treatment of the chlorothalonil aqueous solution improved the biodegradability (BOD_5/COD ratio) from zero to 0.42, indicating that the

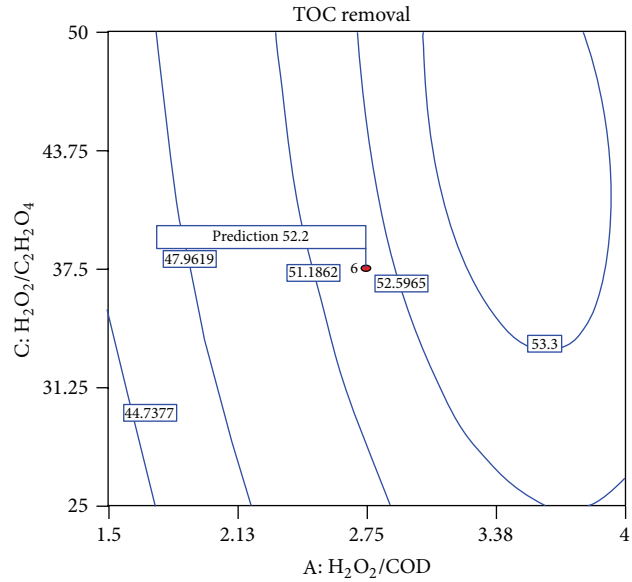

FIGURE 4: Contour plot for TOC removal.

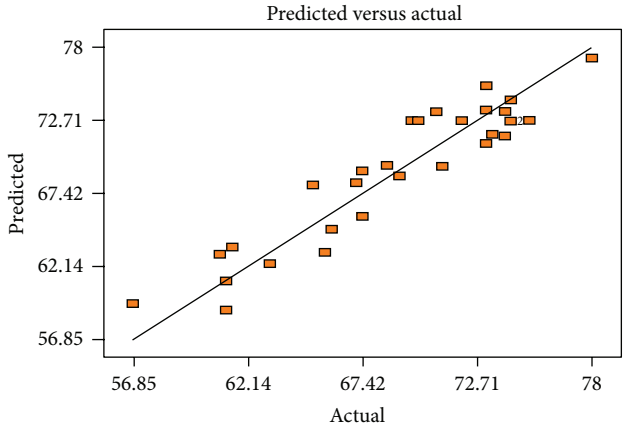

Figure 5: Plot of the predicted versus actual COD removal.

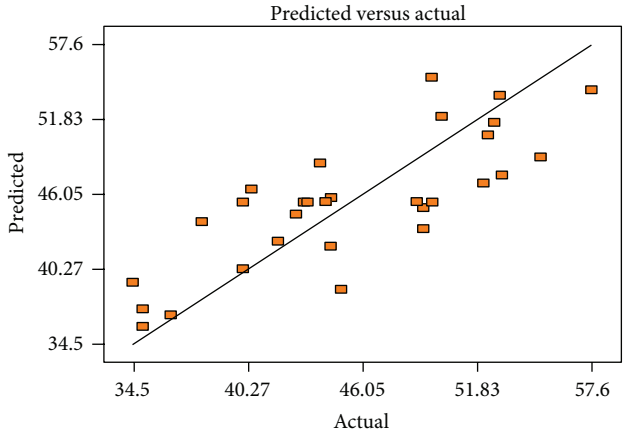

Figure 6: Plot of predicted versus actual NH_3-N removal.

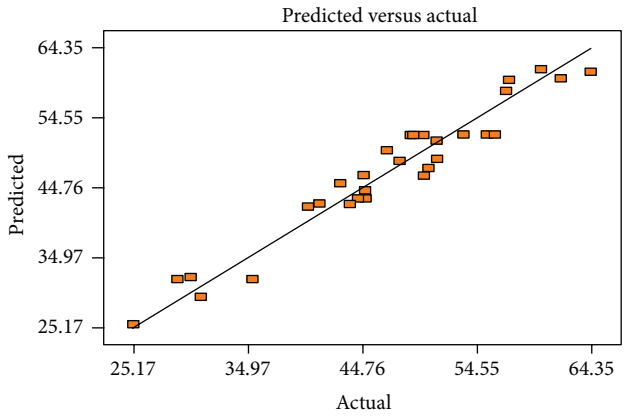

Figure 7: Plot of predicted versus actual TOC removal.

treated pesticide aqueous solution was amenable to biological treatment [33].

3.5. Prospective Application. Complete depollution of pesticide (herbicide) aqueous solution by photoelectro-Fenton or electro-Fenton using boron-doped diamond electrode has been reported [34, 35]. However, solar ferrioxalate/H_2O_2 is a simple energy-efficient process and can be applied as pretreatment of pesticide wastewater to improve biodgradability for subsequent biological treatment.

Table 3: Model prediction and actual removal.

Parameter	Prediction	Actual	% Error
COD removal (%)	72.71	75.71	3.96
NH_3-N removal (%)	45.47	47.11	3.48
TOC removal (%)	52.20	54.33	3.90

4. Conclusions

Visible light-responsive photocatalyst ferrioxalate and H_2O_2 under solar irradiation is effective in degradation of the pesticide chlorothalonil. The optimum operating conditions for solar ferrioxalate/H_2O_2 treatment of a 300 mg/L chlorothalonil aqueous solution obtained by using the central composite design of the response surface methodology were H_2O_2/COD molar ratio 2.75, H_2O_2/Fe^{3+} molar ratio 75, $H_2O_2/C_2H_2O_4$ molar ratio 37.5, reaction time 90 min, and pH 3. Under optimum operating conditions, 75.71, 47.11, and 54.33% removal of COD, NH_3-N, and TOC, respectively was achieved and the biodegradability (BOD_5/COD ratio) improved from zero to 0.42. Model prediction and actual removal were in close agreement. The solar ferrioxalate/H_2O_2 process is effective in pretreatment of chlorothalonil aqueous solution for biological treatment.

Acknowledgment

The authors are thankful to the management and authorities of the Universiti Teknologi PETRONAS for providing facilities for this research.

References

[1] J. W. Kwon and K. L. Armbrust, "Degradation of chlorothalonil in irradiated water/sediment systems," *Journal of Agricultural and Food Chemistry*, vol. 54, no. 10, pp. 3651–3657, 2006.

[2] C. Cox, "Fungicide fact sheet: chlorothalonil," *Journal of Pesticide Reform*, vol. 17, no. 4, pp. 14–20, 1997.

[3] USGS Scientific Investigations Report 2008–5016, "Occurrence of chlorothalonil, its transformation products, and selected other pesticides in Texas and Oklahoma streams, 2003-2004," http://pubs.usgs.gov/sir/2008/5016/pdf/SIR08-5016.pdf.

[4] G. I. Scott, M. H. Fulton, E. F. Wirth et al., "Toxicological studies in tropical ecosystems: an ecotoxicological risk assessment of pesticide runoff in South Florida estuarine ecosystems," *Journal of Agricultural and Food Chemistry*, vol. 50, no. 15, pp. 4400–4408, 2002.

[5] R. D. Wauchope, W. C. Johnson, and H. R. Sumner, "Foliar and soil deposition of pesticide sprays in peanuts and their washoff and runoff under simulated worst-case rainfall conditions," *Journal of Agricultural and Food Chemistry*, vol. 52, no. 23, pp. 7056–7063, 2004.

[6] K. H. Leong, L. L. Benjamin Tan, and A. M. Mustafa, "Contamination levels of selected organochlorine and organophosphate

pesticides in the Selangor River, Malaysia between 2002 and 2003," *Chemosphere*, vol. 66, no. 6, pp. 1153–1159, 2007.

[7] N. Somchit, M. N. Somchit, S. A. Hadi, and M. P. Zakaria, "Persistent organic chemicals in Malaysian waters: a review," *Research Journal of Environmental Toxicology*, vol. 3, no. 2, pp. 101–112, 2009.

[8] M. Sakai, "Determination of pesticides and chronic test with daphnia magna for rainwater samples," *Journal of Environmental Science and Health*, vol. 37, no. 3, pp. 247–254, 2002.

[9] L. L. McConnell, J. LeNoir, S. Datta, and J. Seiber, "Wet deposition of current-use pesticides in the Sierra Nevada mountain range, California, USA," *Environmental Toxicology and Chemistry*, vol. 17, no. 10, pp. 1908–1916, 1998.

[10] D. C. G. Muir, C. Teixeira, and F. Wania, "Empirical and modeling evidence of regional atmospheric transport of current-use pesticides," *Environmental Toxicology and Chemistry*, vol. 23, no. 10, pp. 2421–2432, 2004.

[11] K. Harada, T. Hisanaga, and K. Tanaka, "Photocatalytic degradation of organophosphorus compounds in semiconductor suspension," *New Journal of Chemistry*, vol. 11, no. 8-9, pp. 597–600, 1987.

[12] K. Harada, T. Hisanaga, and K. Tanaka, "Photocatalytic degradation of organophosphorus insecticides in aqueous semiconductor suspensions," *Water Research*, vol. 24, no. 11, pp. 1415–1417, 1990.

[13] D. Barceló, "Environmental Protection Agency and other methods for the determination of priority pesticides and their transformation products in water," *Journal of Chromatography*, vol. 643, no. 1-2, pp. 117–143, 1993.

[14] A. A. Sharbidre, V. Metkari, and P. Patode, "Effect of diazinon on acetylcholinesterase activity and lipid peroxidation of poecilia reticulata," *Research Journal of Environmental Toxicology*, vol. 5, no. 2, pp. 152–161, 2011.

[15] M. Pera-Titus, V. García-Molina, M. A. Baños, J. Giménez, and S. Esplugas, "Degradation of chlorophenols by means of advanced oxidation processes: a general review," *Applied Catalysis B*, vol. 47, no. 4, pp. 219–256, 2004.

[16] J. Kiwi, C. Pulgarin, and P. Peringer, "Effect of Fenton and photo-Fenton reactions on the degradation and biodegradability of 2 and 4-nitrophenols in water treatment," *Applied Catalysis B*, vol. 3, no. 4, pp. 335–350, 1994.

[17] J. P. Scott and D. F. Ollis, "Integration of chemical and biological oxidation processes for water treatment: review and recommendations," *Environmental Progress*, vol. 14, no. 2, pp. 88–103, 1995.

[18] C. Walling, "Fenton's reagent revisited," *Accounts of Chemical Research*, vol. 8, no. 4, pp. 125–131, 1975.

[19] J. J. Pignatello, D. Liu, and P. Huston, "Evidence for an additional oxidant in the photoassisted Fenton reaction," *Environmental Science and Technology*, vol. 33, no. 11, pp. 1832–1839, 1999.

[20] A. Safarzadeh-Amiri, J. R. Bolton, and S. R. Cater, "Ferrioxalate-mediated photodegradation of organic pollutants in contaminated water," *Water Research*, vol. 31, no. 4, pp. 787–798, 1997.

[21] K. A. Hislop and J. R. Bolton, "The photochemical generation of hydroxyl radicals in the UV-vis/ferrioxalate/H_2O_2 system," *Environmental Science and Technology*, vol. 33, no. 18, pp. 3119–3126, 1999.

[22] N. Zhang, J. Huang, and W. Zheng, "Research on photo degradation of aniline wastewater by dynamic UV-vis/H_2O_2/Ferrioxalate complexes process," *Journal of Chemical Industry and Engineering*, vol. 53, no. 1, pp. 36–39, 2002.

[23] P. Tripathi and M. Chaudhuri, "Decolourisation of metal complex azo dyes and treatment of a dyehouse waste by modified photo-Fenton (UV-vis/ferrioxalate/H_2O_2) process," *Indian Journal of Engineering and Materials Sciences*, vol. 11, no. 6, pp. 499–504, 2004.

[24] M. Chaudhuri and T. Y. Wei, "Decolourisation of reactive dyes by modified photo-fenton process under irradiation with sunlight," *Nature Environment and Pollution Technology*, vol. 8, no. 2, pp. 359–363, 2009.

[25] J. M. Monteagudo, A. Durán, J. M. Corral, A. Carnicer, J. M. Frades, and M. A. Alonso, "Catalytic degradation of Orange II in a ferrioxalate-assisted photo-Fenton process using combined UV-A/C-solar pilot-plant system," *Applied Catalysis B*, vol. 951-952, pp. 120–129, 2010.

[26] J. M. Monteagudo, A. Durán, M. Aguirre, and I. San Martín, "Optimization of the mineralization of a mixture of phenolic pollutants under a ferrioxalate-induced solar photo-Fenton process," *Journal of Hazardous Materials*, vol. 185, no. 1, pp. 131–139, 2011.

[27] *Standard Methods for the Examination of Water and Wastewater*, APHA, AWWA and EWF, Washington, DC, USA, 21st edition, 2005.

[28] I. Talinli and G. K. Anderson, "Interference of hydrogen peroxide on the standard COD test," *Water Research*, vol. 26, no. 1, pp. 107–110, 1992.

[29] Y. W. Kang, M. J. Cho, and K. Y. Hwang, "Correction of hydrogen peroxide interference on standard chemical oxygen demand test," *Water Research*, vol. 33, no. 5, pp. 1247–1251, 1999.

[30] *Water Analysis Handbook*, Hach Company, Loveland, Colo, USA, 4th edition, 2002.

[31] Design-Expert Software, Version 6.0.7, User's Guide, 2002.

[32] M. A. Bezerra, R. E. Santelli, E. P. Oliveira, L. S. Villar, and L. A. Escaleira, "Response surface methodology (RSM) as a tool for optimization in analytical chemistry," *Talanta*, vol. 76, no. 5, pp. 965–977, 2008.

[33] F. Al-Momani, E. Touraud, J. R. Degorce-Dumas, J. Roussy, and O. Thomas, "Biodegradability enhancement of textile dyes and textile wastewater by VUV photolysis," *Journal of Photochemistry and Photobiology A*, vol. 153, no. 1-3, pp. 191–197, 2002.

[34] B. Boye, M. M. Dieng, and E. Brillas, "Anodic oxidation, electro-Fenton and photoelectro-Fenton treatments of 2,4,5-trichlorophenoxyacetic acid," *Journal of Electroanalytical Chemistry*, vol. 557, pp. 135–146, 2003.

[35] E. Brillas, B. Boye, I. Sirés et al., "Electrochemical destruction of chlorophenoxy herbicides by anodic oxidation and electro-Fenton using a boron-doped diamond electrode," *Electrochimica Acta*, vol. 49, no. 25, pp. 4487–4496, 2004.